

## Original Article

# Relationship between infiltrating lymphocytes in cancerous ascites and dysfunction of Cajal mesenchymal cells in the small intestine

Xiuli Wang<sup>1</sup>, Jing Li<sup>1</sup>, Duanyang Liu<sup>1</sup>, Lei Zhang<sup>1</sup>, Baoshan Zhao<sup>2</sup>, Jing Tang<sup>1</sup>, Meisi Yan<sup>1</sup>, Dan Kong<sup>3</sup>, Xiaoming Jin<sup>1</sup>

<sup>1</sup>Department of Pathology, Harbin Medical University, Harbin, Heilongjiang, P. R. China; <sup>2</sup>Department of Pathology, Harbin Medical University, Daqing, Heilongjiang, P. R. China; <sup>3</sup>Department of Gynecology, Third Affiliated Hospital of Harbin Medical University, Harbin, Heilongjiang, P. R. China

Received January 26, 2018; Accepted March 12, 2018; Epub April 1, 2018; Published April 15, 2018

**Abstract:** Malignant ascites changes the microenvironment of the peritoneal cavity and damages abdominal functional host cells such as interstitial cells of Cajal (ICC), causing gastrointestinal dysfunction and poor prognosis. Besides tumor cells, malignant ascites contains large numbers of lymphocytes and macrophagocytes. These inflammatory cells act as a 'double arrow' and it is not clear whether they cause injury to ICCs. Our study demonstrates the presence of T lymphocytes in malignant ascites and shows that these cells may have a critical role in inducing damage to ICC via Caspases and Fas/FasL. These inflammatory cells were contributory to gastric dysfunction in our GI tumor-induced ascites mouse models.

**Keywords:** Malignant ascites, interstitial cells of Cajal, tumor associated lymphocytes, gastrointestinal dysfunctions, apoptosis

## Introduction

Malignant ascites is a fatal complication that develops in advanced malignant abdominal tumors [1]. Metastasis of tumors to the abdomen changes the internal environment of the peritoneal cavity, possibly promoting continued growth of tumor cells in ascites in the new microenvironment [2, 3]. How these malignant tumor cells in ascites affect intrinsic cells of abdominal organs, such as functional cells promoting small intestinal motility, is not well understood. Furthermore, it remains uncertain how the altered internal environment impacts the function of these innate tissues and cells. Our group previously demonstrated that gastric cancer patients experiencing peritoneal metastasis show symptoms of intestinal obstruction such as abdominal distension after eating, intermittent abdominal pain, nausea, and vomiting. Investigation in mouse models of malignant peritoneal metastasis has provided evidence that a decrease in the number or function of ICCs potentially contributes to

these motility and stagnation disorders [4]. Cancerous ascites in patients is often accompanied with clinical manifestations of gastrointestinal motility dysfunction which interferes with their treatment. The cause of these symptoms, however, is unknown.

Previous studies have reported that the major population of cells in malignant ascites constitutes tumor cells, tumor-infiltrating lymphocytes, and tumor associated macrophages [5, 6]. The aim of this study was to determine whether these cells negatively impact small intestinal ICC, either directly or indirectly, thereby causing gastrointestinal dysfunction.

## Materials and methods

### *Ethics statement*

Animals were treated in accordance with guidelines for animal experiments at National Cancer Center of China. Study protocol was approved by the Ethics Committee of Harbin Medical

## Infiltrating lymphocytes and dysfunction of Cajal mesenchymal cells

University (Permit Number: HMUIRB20140022). All surgery was performed under amobarbital sodium anesthesia and efforts were made to minimize animal suffering.

### *Reagents and antibodies*

C57BL/6 mice were obtained from Liaoning Biological Technology. Murine foregastric carcinoma (MFC) cells were purchased from Type Culture Collection of the Chinese Academy of Sciences (Shanghai, China). Dulbecco's Modified Eagle's medium (DMEM; Hyclone, USA) was used. Monoclonal anti-mouse CD4, CD8, c-kit, Fas, FasL, caspase-3, caspase-8, and caspase-9 antibodies were obtained from Santa Cruz Biotechnology (Dallas, TX). Fluorescein isothyanate (FITC)-conjugated anti-CD4 and phycoerythrin (PE)-conjugated anti-CD8 were purchased from Biolegend (San Diego, CA). The terminal deoxynucleotidyl transferase-mediated dUTP nick-end labeling (TUNEL) Apoptosis Assay Kit and First Strand cDNA Synthesis Kit were purchased from Roche Diagnostics. SYBR Premix Ex Taq (perfect real time) was purchased from Takara (Mountain View, CA).

### *Cell culture*

MFC cells were grown in Dulbecco's Modified Eagle's medium (DMEM; Hyclone, USA) and supplemented with 10% fetal bovine serum, 100 U/ml penicillin, and 100 mg/ml streptomycin sulfate at 37°C in a 5% CO<sub>2</sub> incubator.

### *Animal models*

Seventy male C57BL/6 mice (4-6 weeks old, 18-20 g) were housed at room temperature (RT, 25°C) with a 12 hour light/dark cycle. Food and water were provided ad libitum. Mice were divided into four groups; three groups of mice, each containing 20 mice, were used to develop peritoneal metastasis model and were sacrificed at 14, 21, or 28 days post-peritoneal tumor inoculation. For these groups of mice, the abdomen was sterilized using iodophor and mice were injected with 1×10<sup>6</sup> MFC cells in 0.2 mL, intraperitoneally. Ten mice, injected with physiological saline (0.9% NaCl) at the same volume, served as control group.

### *Flow cytometry analysis*

Cells from ascitic fluid were adjusted to 1×10<sup>6</sup>/mL and washed twice with fluorescence acti-

vated cell sorting (FACS) buffer (PBS, 2% bovine serum albumin and 0.1% NaN<sub>3</sub>). The cells were subsequently incubated with FITC-anti-CD4 and PE-anti-CD8 antibodies in the dark for 30 minutes on ice. They were then incubated with Red Blood Cell Lysis Buffer (Beyotime, China) for 20 minutes. After washing 3 more times, labeled cells were fixed with 1% formaldehyde solution and proportion of CD4/CD8 in ascites was analyzed using flow cytometry.

### *Enzyme-linked immunosorbent assay (ELISA)*

Antibody solutions specific for CD4, CD8, Fas, FasL, caspase-3, caspase-8, and caspase-9 were diluted 1:1000 and individually conjugated to the flat bottom of a 96-well plate by incubation at 4°C overnight. Plates were washed thrice with phosphate buffered saline-tween (PBS-T) followed by blocking with 1% BSA for 1 hour at room temperature (RT). After washing three times in TBS-T, protein marker and ascites fluid (diluted 1:10) were added to each test well and control. After one hour of incubation at 37°C, ascites was removed and wells were washed with PBS-T and then incubated with HRP-conjugated goat anti-mouse IgG diluted in PBS-T at 37°C for 1 hour. Tetramethylbenzidine (TMB) substrate solution was added to each well and incubated in the dark at RT for 15 minutes. The reaction was terminated with sulphuric acid. Substrate and conjugate controls were included in each plate. Optical density (OD) values were read in a Multiskan ELISA reader (Bio-Rad, Tokyo, Japan) with a 450 nm reference filter.

### *Myoelectrical activity*

Mice were anesthetized with amobarbital sodium and the abdomen was opened with a midline longitudinal incision approximately 2 cm in length. Two bipolar platinum electrodes were placed on the lumen with an interval of 1 cm along the long axis direction of the anti-mesenteric border. Intestinal myoelectrical activity was recorded using a multichannel recorder (model RM6240B; Chengdu Instrument Factory) for 20 minutes. The amplifier was set at a cutoff frequency of 30 Hz.

### *Hematoxylin and eosin (HE)*

Mice were sacrificed by disruption of the cervical spine. A fragment of intact proximal intes-

## Infiltrating lymphocytes and dysfunction of Cajal mesenchymal cells

**Table 1.** Sequences of primers used in real-time PCR amplifications

Gene	Primer sequence	
β-actin	5'-GTC CAC CCG CGA GCA CAG CTT CTT-3'	F
	5'-CTT TGC ACA TGC CGG AGC CGT TGT-3'	R
CD4	5'-AAG TCT CGA GCC CTC ATA TAC ACA CA-3'	F
	5'-CTC GGC ACA TGG TGG TCT CCT TGA GC-3'	R
CD8	5'-GTC CGT TTC GCA AGG ATG CT-3'	F
	5'-CCT TCC TGT CTG ACT AGC GG-3'	R
Fas	5'-GCT GCA GAC ATG CTG TGG ATC-3'	F
	5'-TCA CAG CCA GGA GAA TCG CAG-3'	R
FasL	5'-TCC AGG GTG GGT CTA CTT ACT AC-3'	F
	5'-CCC TCT TAC TTC TCC GTT AGG A-3'	R
Caspase-3	5'-TGG GCC TGA AAT ACC AAG TC-3'	F
	5'-AAA TGA CCC CTT CAT CAC CA-3'	R
Caspase-8	5'-GGC CTC CAT CTA TGA CCT GA-3'	F
	5'-GTG TGG TTC TGT TGC TCG AA-3'	R
Caspase-9	5'-GCC AGA GGT TCT CAG ACC AG-3'	F
	5'-TCC CTG GAA CAC AGA CAT CA-3'	R

F: forward, R: reverse.

tine (approximately 1 cm) was excised and rinsed with ice-cold PBS. Specimens were fixed in 4% paraformaldehyde (PFA) for 24 hours, dehydrated with an ethanol gradient, cleared in xylene, and embedded in paraffin. Tissue sections (thickness, 4 μm) were stained with Hematoxylin and Eosin (HE) and studied using light microscopy.

### Electron microscopy

Fragments of intact proximal intestine were fixed with 3% glutaraldehyde for 2 hours at room temperature. After being rinsed in fresh PBS, tissues were fixed in 1% osmium tetroxide for 2 hours at 4°C. Samples were then rinsed with distilled water thrice for 5 minutes, dehydrated in graded ethanol and propylene oxide, and embedded in Araldite. Ultrathin sections were cut with a Reichert ultramicrotome, double-stained with uranyl acetate and lead citrate, and observed with a JEM1200 EX II electron microscope.

### Fluorescence immunocytochemistry

A fragment of intestine was sectioned at 4 μm thickness and washed three times in PBS. Materials were incubated with c-kit antibodies (1:30; Santa Cruz Biotechnology, CA, sc-168) at 4°C overnight. After washing, the tissue was incubated for an additional 1 hour at 37°C with fluorescein isothiocyanate anti-rabbit IgG

(1:200; Vector). A fluorescence microscope (Nikon 800, Japan) was used to detect immunofluorescence reaction products.

### TUNEL detection

Endogenous peroxidase was inactivated by 3% H<sub>2</sub>O<sub>2</sub> for 10 minutes at room temperature and then washed three times with PBS. Sections were permeabilized with 0.1% Triton X-100 for 2 minutes on ice followed by TUNEL for 1 hour at 37°C, then washed three times with PBS. FITC-labeled TUNEL-positive cells were imaged under a fluorescent microscope using 488 nm excitation and 530 nm emission. Cells with green fluorescence were defined as apoptotic cells.

### Quantitative real time-PCR

Tissues were extracted with TRIzol Reagent (Invitrogen), according to manufacturer protocol. RNA concentration was determined by reading absorbance at 260/280 nm ratio ranging from 1.8 to 2.0. To synthesize first strand cDNA, 1.5 μg of the total RNA template was reverse transcribed with AMV-RTase (1st Strand cDNA Synthesis Kit for RT-PCR; Roche). After reverse transcription reaction, the reaction mixture was amplified by quantitative PCR using Light Cycler DNA Master SYBR Green I Kit (Takara, Mountain View, CA) with the gene-specific primers. PCR amplification was carried out at: 95°C for 30 s; followed by 30 cycles -95°C for 30 s, 60°C for 40 s, 72°C for 30 s, and finally 60°C for 5 minutes. For relative comparison of mRNA expression levels, data from real-time PCR was analyzed with a<sup>ΔΔ</sup>Ct method. Primer sequences used are shown in **Table 1**.

### Western blot analysis

Small intestine samples were lysed in RIPA buffer (Beyotime, China). Protein concentration in the supernatant was measured with a BCA protein assay kit (Beyotime, China). An equal amount of the protein was separated by SDS-PAGE and transferred to nitrocellulose membranes (Amersham Biosciences). Membranes were blocked in 5% nonfat milk in Tris-buffered saline (TBS) for 1 hour and then incubated overnight with anti-c-Kit, anti-CD4 (1:200 dilution, rabbit polyclone, Santa Cruz Technologies), anti-CD8 (Abbiotec) or anti-β-actin antibody (eBioscience; diluted 1:10,000). After several

## Infiltrating lymphocytes and dysfunction of Cajal mesenchymal cells

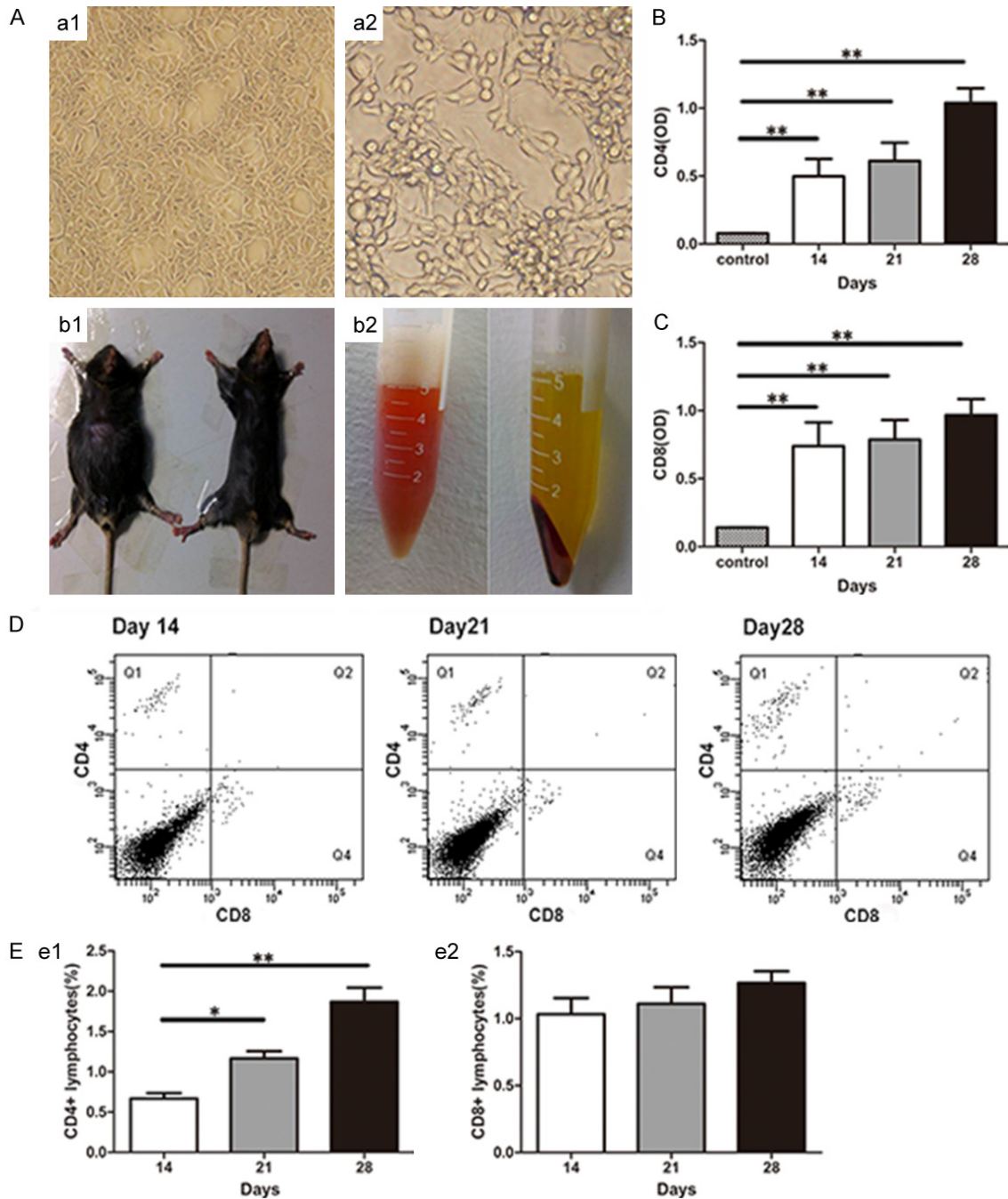


**Figure 1.** Mouse ascites model and flow cytometry analysis of CD4 and CD8. A: (a1, 2) Microscopic images of MFC after 6 days in culture at low (a1, 200 $\times$ ) and high (a2, 400 $\times$ ) magnification. B: (b1) Ascites model given intraperitoneal injection of MFC for 14 days. The left mouse represents the ascites model and the right mouse is the control. (b2) Ascitic fluid from the 14-day model. C: The OD values of CD4 and CD8 in the 14-day, 21-day, and 28-day groups detected using ELISA. D: Representative figures of the flow cytometric analyses of CD4<sup>+</sup> and CD8<sup>+</sup> T lymphocytes. E: Percentages of CD4<sup>+</sup>CD8<sup>+</sup> T lymphocytes in the 14-day, 21-day, and 28-day groups. Bars represent the mean  $\pm$  SD (n=8). (e1) The percentage of CD4<sup>+</sup> T cells was significantly higher in the 28-day ascites group. (e2) The percentage of CD8<sup>+</sup> T cells was increased in all three ascites model groups and there was no significant difference between them (\* $P$ <0.05, \*\* $P$ <0.01).

washes, the blot was incubated with horseradish peroxidase-conjugated secondary antibody-

ies (1:7000) for 1 hour at 37 $^{\circ}$ C. Membranes were detected with the enhanced chemilumi-

## Infiltrating lymphocytes and dysfunction of Cajal mesenchymal cells

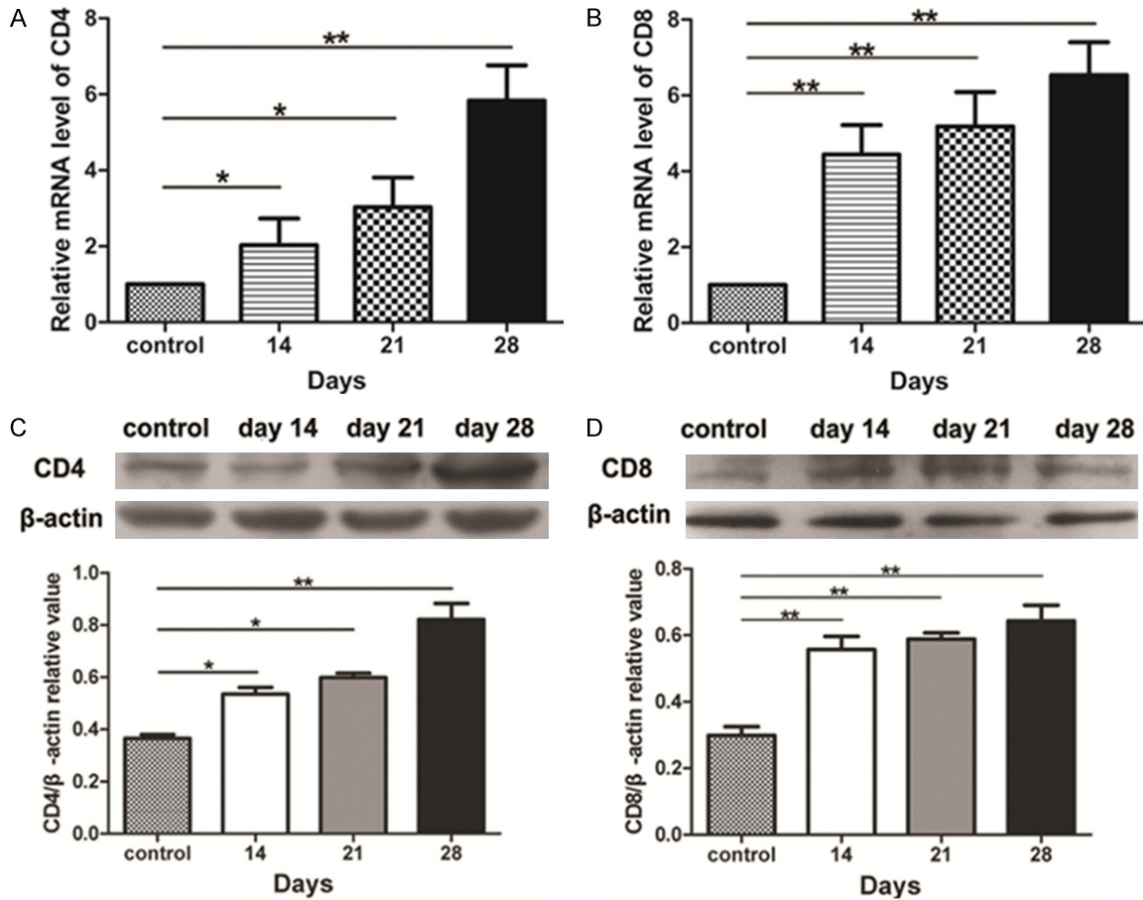


**Figure 2.** Expression of CD4 and CD8 in the intestine. A, B: mRNA levels of CD4 and CD8 were quantified using real-time PCR in intestines of mice from 14, 21, and 28-day groups. C, D: Western blot analysis showed protein expression levels of CD4, CD8, and  $\beta$ -actin. Data were obtained from three independent experiments and expressed as mean  $\pm$  SD.  $n=3$ . \* $P$ , 0.05 versus the control group. \* $P$ <0.05, \*\* $P$ <0.01.

nescence system, according to manufacturer instructions (electrogenenerated chemiluminescence, American Pharmacia).

### Statistical analysis

ANOVA analysis was used to determine the statistical significance of differences between samples. Data are presented as mean  $\pm$  SEM. All statistical tests were two-sided and  $P$  value <0.05 and  $P$ <0.01 indicated an extremely significant difference.

## Results

### Ascites mouse model

Light microscopy showed actively growing adherent MFC cells *in vitro*, compactly arranged in contact with each other (Figure 1A). Mice injected with MFC cells showed formation of ascites at 14 days which continued to develop until 28 days. The ascites was collected and

centrifuged to obtain the supernatant (Figure 1B).

### Activated CD4<sup>+</sup> T and CD8<sup>+</sup> T cells are present in ascites fluid

We evaluated expression of CD4 and CD8 molecules on T lymphocytes by ELISA and flow cytometry. ELISA showed a significant increase ( $P$ <0.01) of both CD4 and CD8 expression in malignant ascites fluid obtained from mice injected with MFC cells, compared to control group's ascitic fluid. Interestingly, OD values of CD4 in the 28-day group were obviously higher than those in the other two groups ( $P$ <0.01, Figure 1C). A representative analysis of lymphocyte subset population by flow cytometry is shown in Figure 1D. Fluorescence activated cell sorting (FACS) analysis of 7-, 14-, and 21-day malignant ascitic fluid showed enriched populations of CD4<sup>+</sup> T lymphocytes with up to

## Infiltrating lymphocytes and dysfunction of Cajal mesenchymal cells

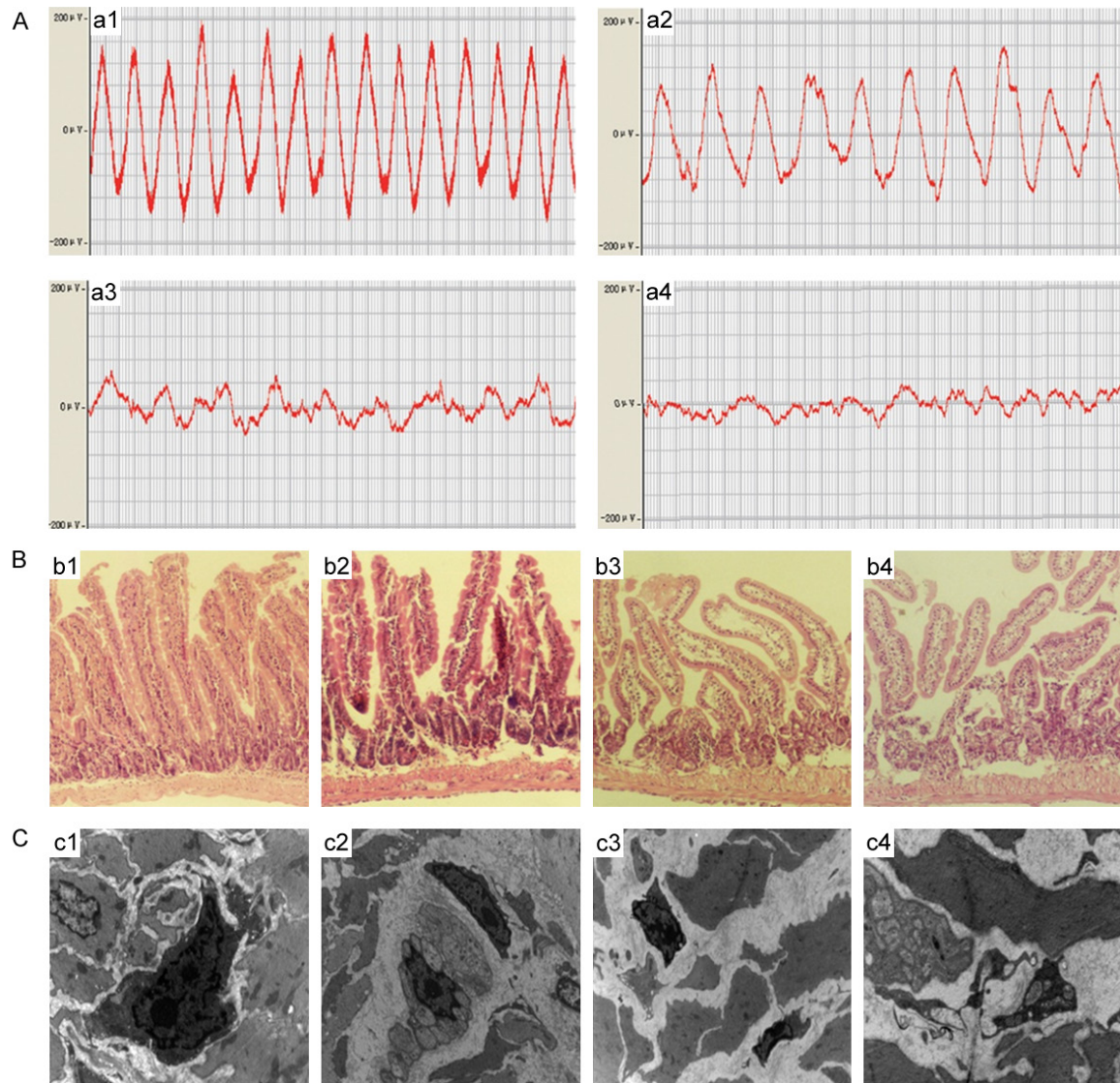


**Figure 3.** Representative photomicrographs of pathological features in intestine. A: The results of electrophysiology analysis of the small intestine of model mice showed weakened peristalsis, decreased amplitude, and reduced frequency compared with the control group, with the model 28-day group showing especially notable decreases. B. b1: The small intestines of the control group had intact villi and the muscularis was of uniform thickness (HE×200). b2: As observed, intestinal villi were not completely intact; submucosa and muscularis showed evidence of edema in the 14-day group mice (HE×200). b3: Small intestines of the 21-day group mice exhibited edematous villi and thinning or uneven thickness of muscle layers (HE×200). b4: Small intestinal muscularis was observed to be thinner and villi were detached in mice in the 28-day group (HE×200). C. Ultrastructural changes of ICC. c1: In control mice intestines, the nucleus was located as expected in the cytoplasm of ICC, organelles were maintained in the cytoplasm, and close contacts were formed with cells adjacent to ICC (EM×6000). c2: ICC in the small intestines of the 14-day group showed initiation of pyknosis, significant decreases in cytoplasmic processes, and loss of contact with surrounding cells (EM×5000). c3: The ICC of the small intestines of the 21-day group showed pyknosis, swollen mitochondria, and partial or complete vacuolation of the varicosity content (EM×5000). c4: ICC in the small intestine of the 28-day group showed additional severe degeneration, such as clear pyknosis and depletion of cytoplasmic processes (EM×5000).

1.6% in the 28-day group mice, significantly higher than those in the other two groups ( $P < 0.05$ ). This was in accordance with ELISA results. This shows that the number of CD4<sup>+</sup> T

cells increased in malignant ascites in a time-dependent manner. However, no significant difference of CD8<sup>+</sup> T lymphocyte population was observed between the three groups.

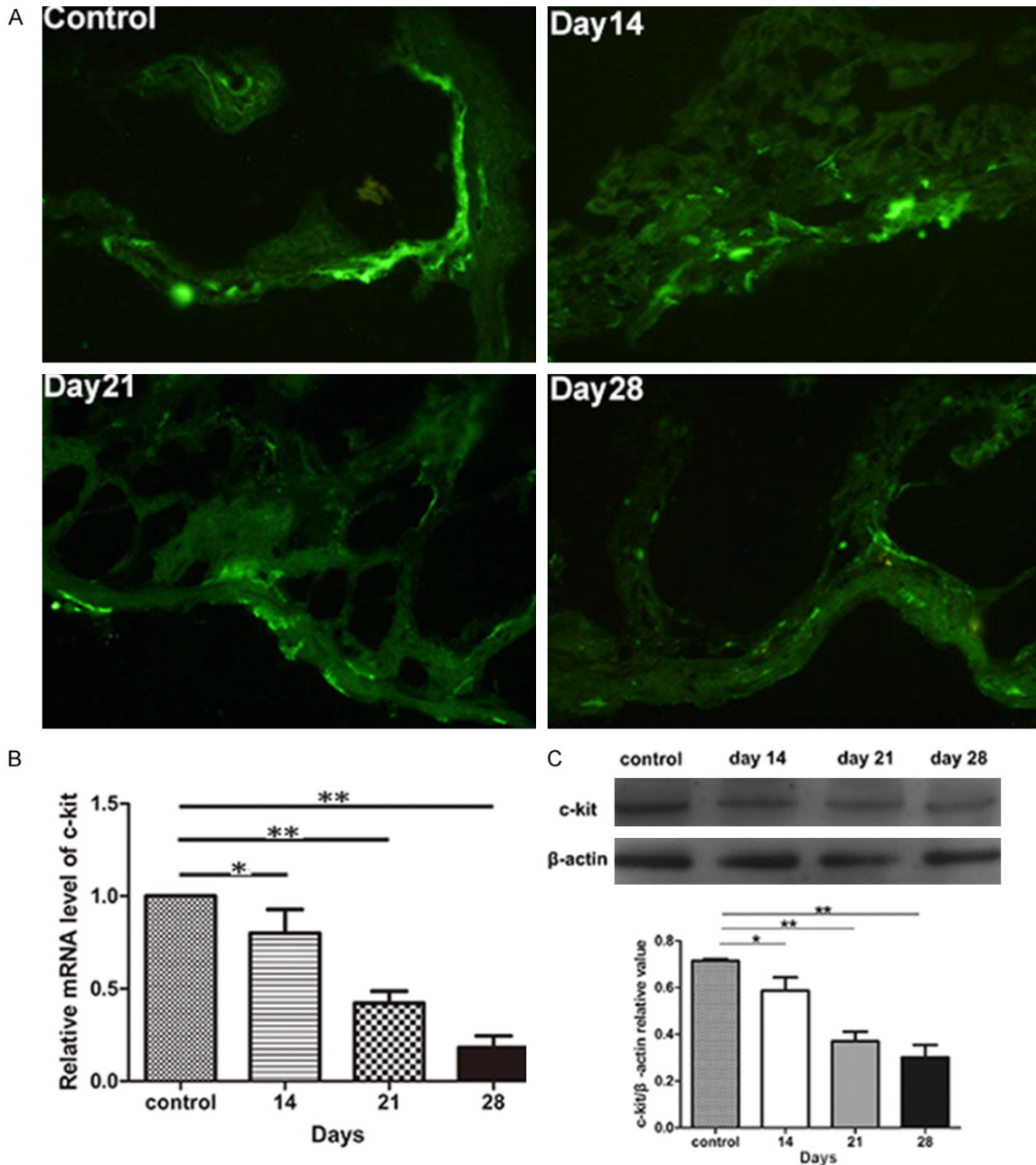


**Figure 4.** Expression of c-kit in intestines. A: In the control group, c-kit expression formed a thick line in control intestinal muscular layers when visualized using immunofluorescence (arrows)  $\times 400$ . As seen, expression of c-kit was rod or decreased, showing discontinuous patterning in the 14-day group (arrows)  $\times 400$ . Expression of c-kit observed as spots and fluorescence intensity is attenuated in the 21-day group (arrows)  $\times 400$ . Expression of c-kit also showed as spots and attenuated fluorescence intensity in the 28-day group (arrows)  $\times 400$ . B: mRNA levels of c-kit quantified using real-time PCR in intestine of model mice at 14, 21, and 28 days after injection of tumor cells or saline ( $n=8$ ). C: Western blot analysis was performed to assess expression of c-kit and  $\beta$ -actin. Data were obtained from three independent experiments and expressed as mean  $\pm$  SD.  $n=3$ . For comparison with the control group,  $*P<0.05$ ,  $**P<0.01$ .

*Expression profiles of CD4 and CD8 in intestinal tissues*

To determine how the host adaptive immune system reacts to malignant ascites *in vivo*,

mRNA expression levels of CD4 and CD8 on T lymphocytes were measured in 14, 21, and 28-day group mice. mRNA levels of CD4 were clearly increased compared with corresponding control group ( $n=8$ ,  $P<0.05$ ). mRNA levels

## Infiltrating lymphocytes and dysfunction of Cajal mesenchymal cells

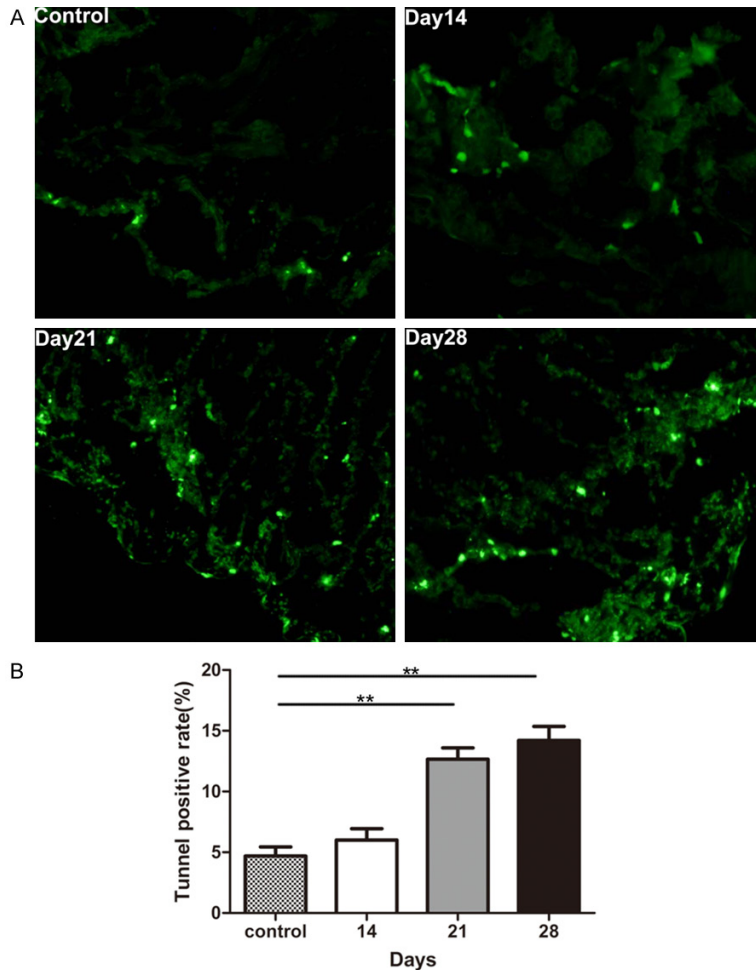


**Figure 5.** Apoptosis in intestines detected using TUNEL assays. A: The tissues were TdT-UTP nick end labeled and imaged via fluorescence microscope (IF×200). B: TUNEL-positive cells are represented by the number of green points in each photograph. All values are denoted as the mean ± SEM from eight independent photographs for each group. n=6. \* $P<0.05$ .

remained on an upward trend until the 28-day group, which showed significantly higher levels than other groups (n=8,  $P<0.01$ , **Figure 2A**). Moreover, mRNA levels of CD8 were significantly increased in all ascites models (n=8,  $P<0.01$ ) and there were no statistically significant differences between the groups (**Figure 2B**). Western blot analysis (**Figure 2C**) showed that CD4 protein in intestinal tissues from the 14, 21, and 28-day group was significantly higher than controls ( $0.54\pm 0.03$ ,  $0.6\pm 0.02$  and  $0.82\pm 0.06$  vs  $0.37\pm 0.01$  respectively, all  $P<0.01$ ). Also, expression of CD4 was seen to increase with time (28 days >21 days >14 days), post-inoculation. Western blot results for CD8 were in accordance with real time PCR results. Compared to control group ( $0.30\pm$

$0.03$ ), CD8 expression was significantly decreased in 14-day group ( $0.56\pm 0.04$ ), 21-day group ( $0.59\pm 0.02$ ), and 28-day group ( $0.52\pm 0.14$ , all  $P<0.01$ ) (**Figure 2D**).

### Morphological analysis

The frequency of peristalsis and amplitude in malignant ascites groups had decreased compared to the control group. The 28-day group showed particularly reduced values (**Figure 3A**). In the control group, small intestine epithelium microvilli were neatly arranged, glands of lamina propria maintained their integrity, and muscularis propria thickness was uniform (**Figure 3b1**). HE staining of the small intestine from peritoneal metastasis model mice showed swelling, decrease in villus height, and increased thickness in muscle layers of the proximal bowel (**Figure 3b2-b4**). Electron microscopy of the intestines of control mice showed the nucleus in cytoplasm of the interstitial cells of Cajal (ICC), as expected for healthy cells. An abundance of functional cytoplasmic processes and close connections between neighboring

cells were visible (**Figure 3c1**). However, early stages of ascites formation was accompanied by vacuolation in ICC, a decrease in volume (**Figure 3c2**), and most ICC had lost synapse-like connections with surrounding cells. Cell content was partially depleted and pyknosis was frequently observed within cell bodies (**Figure 3c3, 3c4**).

### Changes in c-kit levels

Immunofluorescence assays revealed a strip of c-kit expression in the control mice intestinal muscular layer. Expression of c-kit was decreased or attenuated in all three ascites model groups over time, appearing as a dotted or grainy structure in the 14 and 21-day group mice. c-kit immunoreactivity was significantly

## Infiltrating lymphocytes and dysfunction of Cajal mesenchymal cells

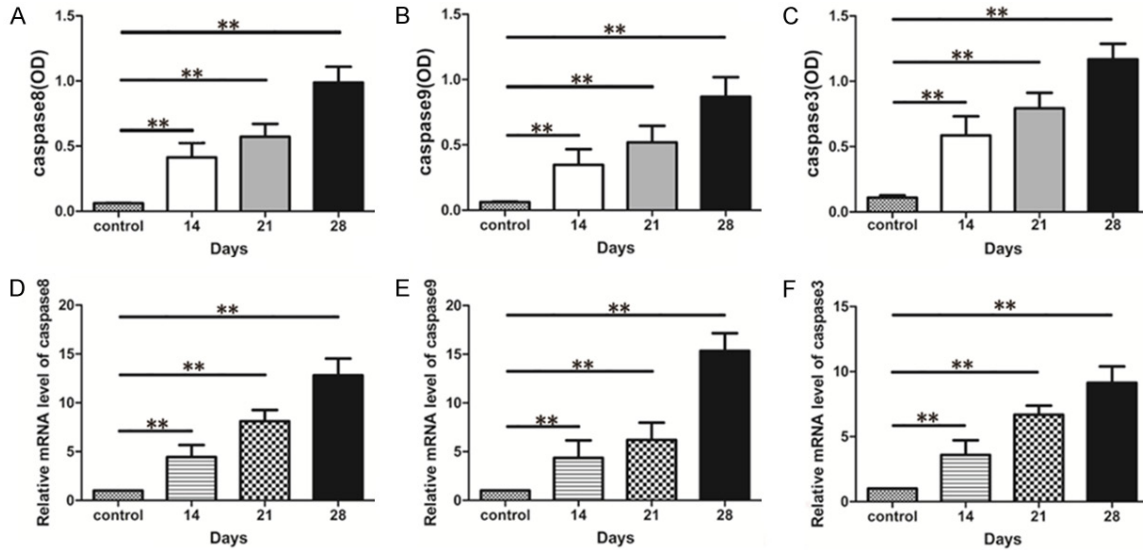


**Figure 6.** Expression profiles of caspase-8, caspase-9, and caspase-3. A-C: The OD values of caspase-8, caspase-9, and caspase-3 were significantly increased in the 14-, 21-, and 28-day model groups. D-F: Real-time PCR measurements of mRNA expression of caspase-8, caspase-9, and caspase-3 in 14-, 21-, and 28-day model groups. The mRNA levels of caspase-8, caspase-9, and caspase-3 were significantly higher than those in the control group. n=8, \* $P<0.05$ , \*\* $P<0.01$ .

weakened in the 28-day group (Figure 4A). c-kit mRNA levels in malignant ascites from 14-days group mice, measured by real-time PCR, showed a significant decrease in expression compared to the control group. This decrease in c-kit mRNA expression in the ascites further decreased towards 21- and 28-day group mice (Figure 4B). Western blot analysis also showed a similar decrease in c-kit expression in malignant ascites, compared to control group. Compared with the control group ( $0.72\pm 0.006$ ), c-kit expression was significantly decreased in 14-day group ( $0.58\pm 0.05$ ), 21-day group ( $0.37\pm 0.04$ ), and 28-day group ( $0.30\pm 0.05$ , all  $P<0.01$ ) (Figure 4C).

### TUNEL assay of apoptosis

Apoptosis was detected using TUNEL assay. Few TUNEL-positive cells were observed in the small intestinal mucosal muscularis of control group mice. TUNEL-positive cells of 14-day group ( $5.37\pm 0.92$ ) showed slightly higher levels than the control group ( $4.3\pm 0.68$ ) but the difference was not statistically significant (Figure 5A). There was, however, a significant increase in number of TUNEL-positive cells in the 21 ( $13.49\pm 0.81$ ) and 28-day groups ( $15.17\pm 0.64$ ) compared to the control group ( $4.3\pm 0.68$ , Figure 5A). No significant difference was observed between these two groups (Figure 5B).

### Expression profiles of caspase-8, caspase-9, and caspase-3

ELISA analysis revealed that OD values for caspase-8, caspase-9, and caspase-3 in ascites mouse model groups showed statistically significant increases relative to the control group ( $P<0.01$ , Figure 6A-C). Real-time PCR showed that levels of caspase-8, caspase-9, and caspase-3 mRNA were elevated, relative to the control group, and increased as the days of ascites formation increased. mRNA levels of caspase-8, caspase-9, caspase-3 were increased in the 14-day ( $P<0.05$ ) and more significantly in 21- and 28-day ascites group mice compared to control ( $P<0.01$ , Figure 6D-F).

### Expression profile of Fas and FasL

Levels of Fas and FasL were determined using ELISA. As shown in Figure 7, OD values in ascites model groups were clearly higher than in the control ( $P<0.01$ , Figure 7A, 7B). Furthermore, we detected that Fas and FasL mRNA levels were significantly increased compared to control group (Figure 7C, 7D).

## Discussion

Ascites contains a rich tumor-friendly microenvironment that not only promotes tumor growth but also causes changes in organs and impor-

## Infiltrating lymphocytes and dysfunction of Cajal mesenchymal cells

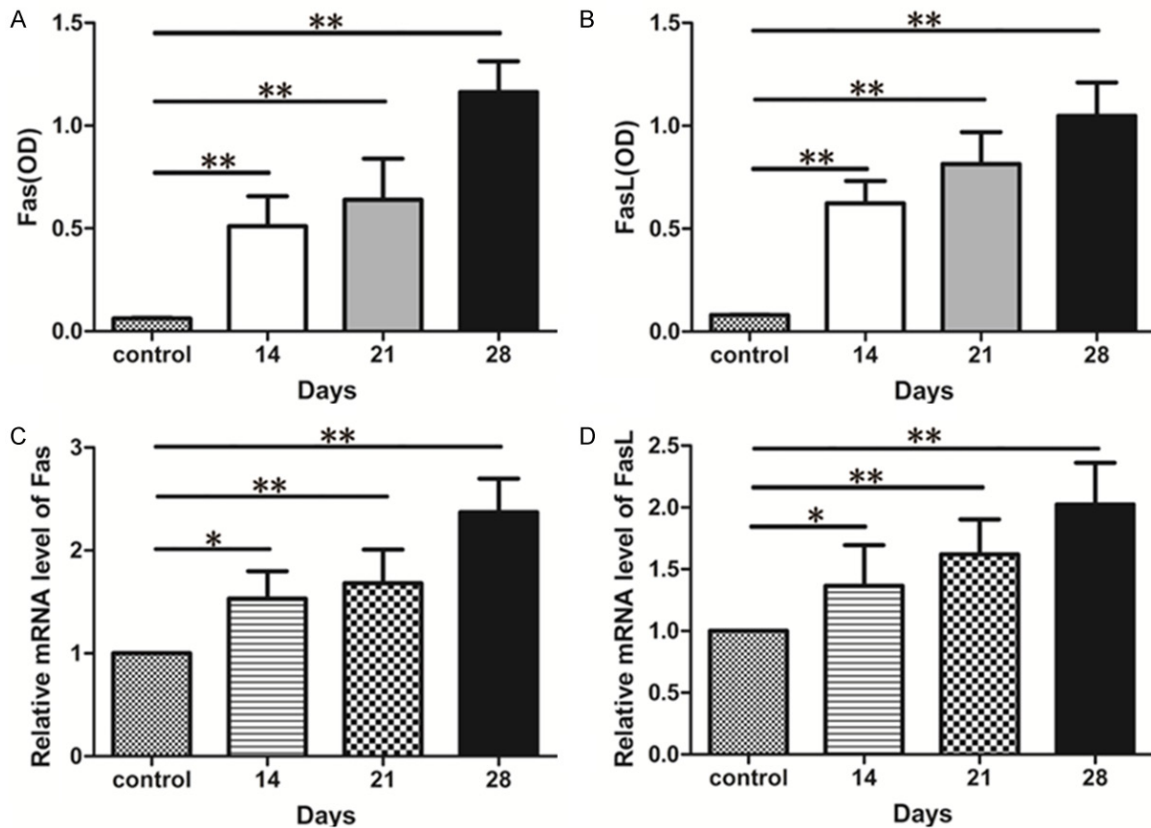


**Figure 7.** Expression profiles of Fas and FasL. A, B: OD values of Fas and FasL were significantly increased in all model groups. C, D: mRNA expression of Fas and FasL were quantified using real-time PCR in the intestines of all three model groups. mRNA levels of Fas and FasL in model groups were significantly higher than in the control group. There were no statistically significant differences between levels in the model groups.  $n=8$ ,  $**P<0.01$ .

tant functional cells of the peritoneal cavity [7, 8]. Interstitial cells of Cajal (ICCs) are pacemaker cells responsible for initiating slow-wave activity in GI muscles and mediation of neural input to smooth muscle cells [9, 10]. Patients diagnosed with peritoneal metastasis or ascites formation show intestinal obstruction symptoms such as abdominal swelling, intermittent abdominal pain, nausea, vomiting, and flatulence. Ascites increases patient morbidity and causes a reduction in quality of life.

The pathogenic mechanism by which peritoneal metastasis and malignant ascites causes gastrointestinal (GI) motor disorders has remained unclear. In previous studies, we developed a peritoneal metastasis mouse model of gastric cancer, involving intraperitoneal injection of mice with gastric cancer cells, to study causes of GI motor disorders. In these mouse models, we observed that amplitude and frequency of intestinal slow waves had signifi-

cantly decreased. Light microscopy showed that the small intestinal musculature became thinner and was infiltrated with inflammatory cells. Ultrastructural injury of ICC could be observed such as decreased cell size, decreased or absent synapse-like contacts, numerous myeloid bodies, and inflammatory infiltrate that included macrophages and lymphocytes. Synapse-like connections between smooth muscle cells and enteric nerves were lost and cellular contents were partially depleted. GI dysfunction induced by peritoneal metastasis of gastric cancer was associated with abnormalities such as depletion in cell numbers, apoptosis, pyknosis, and atypical electrophysiological activity. We hypothesized that ICC abnormalities form the primary basis of gastrointestinal motility dysfunction in this setting [4].

Tissue microarray analysis of malignant ascites showed increased presence of tumor-infiltrating lymphocytes (TILs) and TAMs [11]. These

## Infiltrating lymphocytes and dysfunction of Cajal mesenchymal cells

TILs constituted CD3<sup>+</sup>, CD4<sup>+</sup>, and CD8<sup>+</sup> lymphocytes [12-14]. Microarray analysis of tumor tissues revealed that inflammatory cells and cytokines may play an important role in development and progression of tumors, regulation of angiogenesis and lymphangiogenesis, suppression of the immune response, regulation of extracellular matrix changes, and interactions between stem cells [15, 16]. These inflammatory cells may also play a significant role in functions of abdominal cells, particularly regarding intestinal ICC injury which causes symptoms such as abdominal pain, abdominal distension, intestinal obstruction, and others. These effects may form part of the pathological basis for dysfunctional gastrointestinal motility in patients with advanced gastric cancer. In addition to tumor cells, we observed a significant population of CD4<sup>+</sup> and CD8<sup>+</sup> T lymphocytes in our malignant ascites model. The relationship between T lymphocytes, gastrointestinal dysfunction, and ICC injury is an important unanswered question.

Apoptosis is a tightly integrated, active, and orderly process that maintains a stable cellular environment and is under the control of a variety of important genes. It is an active cellular self-sacrifice mechanism induced to allow better adaptation to the environment. Fas/FasL is one of the most important mechanisms of cell apoptosis. The Fas/FasL system gives priority to membrane receptor death pathways, which play an important role in cell apoptosis. Fas ligand (FasL) belongs to the tumor necrosis factor (TNF) family and induces apoptosis by binding with Fas (CD95/APO-1) receptor-positive cells [17-19]. We reported, here, that gastrointestinal dysfunction caused by malignant ascites may be caused by tumor-infiltrating lymphocytes in ascitic fluid, likely by affecting functional host cells, such as ICC. High levels of caspases 8, 9, 3, and Fas/FasL signaling may play an important role in primary regulation of lymphocytic responses to malignant ascites. Previous studies have shown that nerve cells were easily invaded with tumor infiltrating lymphocytes. Occurrence of nervous tissue infiltration was closely related to presence of CD4<sup>+</sup>, CD8<sup>+</sup>, and Fas<sup>+</sup> tumor-infiltrative lymphocyte subtypes. However, the depth of tissue infiltration was correlated with a reduction in number of CD4<sup>+</sup> T cells and an increase of percentage of CD8/Fas cells [20, 21].

The tumor inflammatory microenvironment is a complicated network due to the large quantities of cytokines as well as inflammatory cells and factors [22]. This complex inflammatory network can influence host cells directly or indirectly by endocrine, exocrine, and paracrine signaling. Tumor-infiltrating lymphocytes and tumor-associated macrophages are important messengers between the inflammatory microenvironment and tumor progression. These messengers enhance neo-angiogenesis and tune the inflammatory response, adaptive immunity, extracellular matrix remodeling, and immunosuppressive action [23-25]. Impairment of intraperitoneal functional cells due to tumor microenvironments, especially damage to ICCs, likely contributes to gastric dysfunction in our GI tumor-induced ascites mouse models.

In conclusion, onset and progression of malignant ascites is associated with advanced gastrointestinal cancer and leads to poor prognosis and a significant reduction in quality of life. Unfortunately, there are no accepted guidelines for management of this condition. Survival time of patients is shortened by complications introduced by the decrease or stagnation of gastrointestinal peristalsis. Here, we report that injury of intestinal ICC, caused by tumor infiltrating lymphocytes in abdominal fluids, is a likely contributor to these symptoms. These findings suggest the need for an adapted therapy at early stages of ascites formation which may alleviate complications and improve quality of life in patients with ascites-associated gastrointestinal cancers.

### Acknowledgements

We would like to thank the National Natural Science Foundation of China (Grant number 81372611, 81301750), the Scientific Research Fund of Harbin Medical University-Daqing (Grant number DQ2013-1), and Research Project of Health and Family Planning Commission of Heilongjiang Province (Grant number 2014-432) for support in completion of this manuscript.

### Disclosure of conflict of interest

None.

**Address correspondence to:** Xiaoming Jin, Department of Pathology, Harbin Medical University, 157

## Infiltrating lymphocytes and dysfunction of Cajal mesenchymal cells

Baojian Road, Nangang District, Harbin, P. R. China.  
Tel: +86-15846160480; E-mail: jinxm55@163.com;  
Dan Kong, Department of Gynecology, Third Affiliated Hospital of Harbin Medical University, 150 Haping Road, Nangang District, Harbin, P. R. China.  
E-mail: 15395030@qq.com

### References

- [1] Saif MW, Siddiqui IA and Sohail MA. Management of ascites due to gastrointestinal malignancy. *Ann Saudi Med* 2009; 29: 369-377.
- [2] Harding V, Fenu E, Medani H, Shaboodien R, Ngan S, Li HK, Burt R, Diamantis N, Tuthill M, Blagden S, Gabra H, Urch CE, Moser S and Agarwal R. Safety, cost-effectiveness and feasibility of daycase paracentesis in the management of malignant ascites with a focus on ovarian cancer. *Br J Cancer* 2012; 107: 925-930.
- [3] Maeda H, Kobayashi M and Sakamoto J. Evaluation and treatment of malignant ascites secondary to gastric cancer. *World J Gastroenterol* 2015; 21: 10936-10947.
- [4] Zheng H, He Y, Tong J, Sun L, Yang D, Li H, Ao N, Jin X and Zhang Q. Is gastrointestinal dysfunction induced by gastric cancer peritoneal metastasis relevant to impairment of interstitial cells of Cajal? *Clin Exp Metastasis* 2011; 28: 291-299.
- [5] Man YG, Stojadinovic A, Mason J, Avital I, Bilchik A, Bruecher B, Protic M, Nissan A, Izadjoo M, Zhang X and Jewett A. Tumor-infiltrating immune cells promoting tumor invasion and metastasis: existing theories. *J Cancer* 2013; 4: 84-95.
- [6] Hwang WT, Adams SF, Tahirovic E, Hagemann IS and Coukos G. Prognostic significance of tumor-infiltrating T cells in ovarian cancer: a meta-analysis. *Gynecol Oncol* 2012; 124: 192-198.
- [7] Bragado P, Sosa MS, Keely P, Condeelis J and Aguirre-Ghiso JA. Microenvironments dictating tumor cell dormancy. *Recent Results Cancer Res* 2012; 195: 25-39.
- [8] Koontongkaew S. The tumor microenvironment contribution to development, growth, invasion and metastasis of head and neck squamous cell carcinomas. *J Cancer* 2013; 4: 66-83.
- [9] Wallace JA, Li F, Leone G and Ostrowski MC. Pten in the breast tumor microenvironment: modeling tumor-stroma coevolution. *Cancer Res* 2011; 71: 1203-1207.
- [10] Chen Y, Shamu T, Chen H, Besmer P, Sawyers CL and Chi P. Visualization of the interstitial cells of cajal (ICC) network in mice. *J Vis Exp* 2011.
- [11] Mohla S and Witz IP. The 5th international conference on tumor microenvironment: progression, therapy and prevention versailles, france, october 20-24, 2009: conference summary. *Cancer Microenviron* 2010; 3: 1-5.
- [12] Kawabata A, Ohta N, Seiler G, Pyle MM, Ishiguro S, Zhang YQ, Becker KG, Troyer D and Tamura M. Naive rat umbilical cord matrix stem cells significantly attenuate mammary tumor growth through modulation of endogenous immune responses. *Cytotherapy* 2013; 15: 586-597.
- [13] Grivennikov SI, Greten FR and Karin M. Immunity, inflammation, and cancer. *Cell* 2010; 140: 883-99.
- [14] Matsumoto H, Thike AA, Li H, Yeong J, Koo SL, Dent RA, Tan PH and Iqbal J. Increased CD4 and CD8-positive T cell infiltrate signifies good prognosis in a subset of triple-negative breast cancer. *Breast Cancer Res Treat* 2016; 156: 237-247.
- [15] Qin LX. Inflammatory immune responses in tumor microenvironment and metastasis of hepatocellular carcinoma. *Cancer Microenviron* 2012; 5: 203-209.
- [16] Ahmed N and Stenvers KL. Getting to know ovarian cancer ascites: opportunities for targeted therapy-based translational research. *Front Oncol* 2013; 3: 256.
- [17] Liu Y, Wang YR, Ding GH, Yang TS, Yao L, Hua J, He ZG and Qian MP. JAK2 inhibitor combined with DC-activated AFP-specific T-cells enhances antitumor function in a Fas/FasL signal-independent pathway. *Onco Targets Ther* 2016; 9: 4425-4433.
- [18] Elmansy H, Kotb A, Hammam O, Abdelraouf H, Salem H, Onsi M and Elleithy T. Prognostic impact of apoptosis marker Fas (CD95) and its ligand (FasL) on bladder cancer in Egypt: study of the effect of schistosomiasis. *Ecancermedicalscience* 2012; 6: 278.
- [19] Akimzhanov AM, Wang X, Sun J and Boehning D. T-cell receptor complex is essential for Fas signal transduction. *Proc Natl Acad Sci U S A* 2010; 107: 15105-15110.
- [20] Li K, Baird M, Yang J, Jackson C, Ronchese F and Young S. Conditions for the generation of cytotoxic CD4(+) Th cells that enhance CD8(+) CTL-mediated tumor regression. *Clin Transl Immunology* 2016; 5: e95.
- [21] von Rossum A, Krall R, Escalante NK and Choy JC. Inflammatory cytokines determine the susceptibility of human CD8 T cells to Fas-mediated activation-induced cell death through modulation of FasL and c-FLIP(S) expression. *J Biol Chem* 2011; 286: 21137-21144.
- [22] Maletzki C and Emmrich J. Inflammation and immunity in the tumor environment. *Dig Dis* 2010; 28: 574-578.
- [23] Ma HY, Liu XZ and Liang CM. Inflammatory microenvironment contributes to epithelial mesenchymal transition ingastriccancer. *World J Gastroenterol* 2016; 22.

## Infiltrating lymphocytes and dysfunction of Cajal mesenchymal cells

- [24] Geremia A, Biancheri P, Allan P, Corazza GR and Di Sabatino A. Innate and adaptive immunity in inflammatory bowel disease. *Autoimmun Rev* 2014; 13: 3-10.
- [25] Tarin D. Clinical and biological implications of the tumor microenvironment. *Cancer Microenviron* 2012; 5: 95-112.